Journal of the Iranian Chemical Society (2023) 20:1007–1022
https://doi.org/10.1007/s13738-023-02742-9

REVIEW

Recent advances in the development of carbon/metal oxides nanohybrids for enhanced H_2S detection: a review

S. Sureshkumar[1] · S. Rajakumari[2] · R. Manonmani[3]

Received: 20 September 2022 / Accepted: 2 January 2023 / Published online: 12 January 2023

Abstract
Hydrogen sulfide (H_2S) is a poisonous gas and corrosive with a characteristic rotten egg smell. Exposure to a higher concentration of H_2S gas leads to death. Research groups across the globe have been working on developing a gas sensor composed of novel sensing materials to monitor deadly H_2S gas for over a decade. Carbon-based materials such as single-wall carbon nanotubes, multi-wall carbon nanotubes, graphene, and graphene derivatives have been incorporated with metal oxides to improve H_2S gas sensing properties. Carbon-based composites have unique physicochemical properties which provide the sensor possessing superior sensitivity, selectivity, stability, quick response time, etc. This review highlights the importance of H_2S sensors based on rGO/MOx and CNT/MOx, their enhanced sensitivity and selectivity to H_2S.

Keywords Hydrogen sulfide · Gas sensor · Carbon-based composites · Graphene

Introduction

Hydrogen sulfide (H_2S) is a colorless, corrosive, and flammable gas characteristic of a foul smell at ppm level. H_2S gas is produced naturally by degrading organic matter by microorganism and geothermal activities, including petroleum refining and natural gas processing. It is used as a process gas in heavy water plants and chemical laboratories [1–3]. People mainly contact H_2S through inhaling, diffusing through the respiratory system, and entering the bloodstream. Exposure to H_2S gas at a higher concentration (> 100 ppm) for more than 10 min would lead to poisoning and sudden death. H_2S can also produce respiratory illness, nausea, vomiting, and nervous problems at very low concentrations [4, 5]. Accordingly, the detection of H_2S is important as safety is a concern. Gas chromatography and mass spectrometry are the major analytical tool for H_2S analysis at very low concentrations [6, 7]. These methods are required highly sophisticated instruments, complicated sampling preparation, and a time-consuming process. Conventional portable sensors have been deployed in industries and residential places to monitor H_2S gas. However, the conventional sensors are not economical and fail to have stability, fast response, and recovery time [8, 9]. Alternatively, several researchers have developed a sensor based on semiconducting nano-oxides (MOx) such as SnO_2 [10], ZnO [11], CuO [12], WO_3 [13], MoO_3 [14], In_2O_3 [15], and Fe_2O_3 [16] for monitoring H_2S, because the sensors are easy to fabricate, have high stability and high sensitivity, have simple operation and fast dynamics, and do not require complicated step while fabrication [2]. These sensors work based on the chemoresistance method, the easiest transducing scheme. The chemiresistive transducing scheme measures the sensor's electrical resistance while interacting with analyte gas molecules in the environment. However, the MOx-based sensor also has some drawbacks, including high operating temperature, less sensing response, and long recovery time [17, 18]. Different methods have been explored to enhance the gas-sensing properties of MOx- based sensors [19–26]. Among them, developing carbon derivatives combined with MOx-based composite has been considered an effective approach to improving H_2S gas sensitivity. Carbon-based materials such as carbon nanotubes (CNT), graphene, and reduced graphene oxide (rGO) have been incorporated into metal oxides to enhance the gas-sensing properties [27–41].

✉ S. Sureshkumar
sureshkumarbhc@gmail.com

[1] Department of Chemistry, Rajalakshmi Engineering College, Chennai, India

[2] Department of Chemistry, Rajalakshmi Institute of Technology, Chennai, India

[3] PG and Research Department of Chemistry, Ethiraj College for Women, Chennai, India

Carbon-based metal oxide composites act as a sensing layer of the sensor to be more stable, selective, quick response recovery in time and work at low operating temperatures, which indirectly reduces the complicated fabrication steps [25, 42]. Carbon-based composite materials have appeared as promising sensing materials for H_2S detection, considering the advantage of electronic properties. Carbon–metal oxide composites have been considered interesting materials for gas-sensing applications for the last decade. The objective of the present review is to give an overview of the H_2S sensor based on carbon composite materials and the major role played by carbonaceous material in the sensing performance of the sensor. H_2S gas sensing mechanism and gas sensing performance of carbon composites are discussed. The gas sensing mechanism of each carbon-based metal oxide nanostructure type has also been addressed. The promising approaches for sensor fabrication for real field application were highlighted.

rGO/ZnO composite sensor for H_2S detection

ZnO has been widely studied as a sensing material for H_2S gas detection due to its intrinsic electronic properties (band gap–3.37 eV), excellent chemical/thermal stability, and quick response time. For the last three decades, ZnO has been widely used as a sensing material for detecting a wide range of toxic gases, including volatile organic compounds, NH3, CO, and H_2S, due to its intrinsic electronic and optical properties [43–45]. Normally, ZnO-based sensors work at temperatures ranging from 400 ℃ to 600 ℃ as they have poor electronic conductivity at low temperature/room temperature. ZnO is often combined with a p-type semiconducting metal oxide to make it a p–n junction interface to obtain a highly sensitive sensor to analyte gas [46–48]. Similarly, the n-type ZnO had been combined with p-type rGO to enhance the gas sensing response by forming the p-n heterojunction interface [27]. Doping with reduced graphene oxide (rGO) enhances the host material's electronic properties. rGO generates a charge transport carrier at the junction and creates more surface-active sites for analyte gas molecules. At the same time, optimizing rGO % in ZnO is crucial as it determines the sensing performance. Further, the excess amount of rGO on host materials might change the crystal lattice of host materials, eventually reducing the sensitivity. For instance, Shen et al. synthesized mesoporous and nanocrystalline rGO/ZnO through a hydrothermal process for H_2S detection [49]. Mesoporous and nano-crystallinity of the materials were confirmed through BET and XRD analysis. The sensor was fabricated by mixing rGO/ZnO with ethyl cellulose and ethanol to make it a rheological paste and drop coated on an alumina ceramic tube and then dried at 60℃. It was reported that rGO/ZnO (5 wt%) exhibited enhanced sensitivity to ZnO. The sensitivity was 55.91 at 160℃ upon exposure to 50 ppm of H_2S, which was 12 times higher than pure ZnO. It was also reported that the sensor's selectivity was achieved depending on the analyte gas polarity, molecular weight, and reactivity. According to this report, the selectivity to H_2S was attributed to the polar nature and strong reducing characteristics of the target gas than other interfering gas molecules. Dang and his team prepared rGO/ZnO nanofibers for H_2S gas detection. The rGO [50] incorporated into ZnO was carried out by internal and external routes, of which the internal junction of rGO/ZnO showed superior gas sensing performance. The optimum working temperature of the sensor was found to be 350 ℃. The sensor had excellent selectivity, and a high response time (1353) to 1 ppm was achieved when doping with 0.1% rGO content.

The electron depletion region of ZnO was wider due to the formation of heterojunction between p-type rGO and n-type ZnO. When the sensor composed of rGO/ZnO was exposed to H_2S, it reacted with adsorbed oxygen and released electrons back into the conduction band, which increased electron conductivity and contributed to the sensor signal. Further, rGO/ZnO was highly selective to H_2S among common interfering gases. The reason is that rGO creates an additional spillover effect on the surface, consequently enhancing the sensor response [51]. However, this justification is inadequate to explain the sensor based on rGO/ZnO, which possesses high sensitivity and selectivity. There should be two additional justifications; first, the bond energy of H_2S (363 kJ mol^{-1}) is low and highly reactive to oxygen ions when compared to other reducing gases H_2 (386 kJ mol^{-1}) and NH_3 (432 kJ mol^{-1}); secondly, the spontaneous sulfuration–desulfuration reaction of ZnO enhances the sensitivity.

$$ZnO + H_2S \rightarrow ZnS + H_2O \quad \Delta G = -68.2 \text{ kJ mol}^{-1}$$
$$2ZnS + 3O_2 \rightarrow 2ZnO + 3SO_2 \quad \Delta G = -820.4 \text{ kJ mol}^{-1}$$

Multidimensional (0D, 1D, and 2D) nanostructure has been developed for gas sensor, and energy storage applications as the materials possess a high surface-to-volume ratio, structural defects, active sites, and increased ionic/electronic properties [52, 53]. Tran Viet Cuong and co-workers developed ZnO nanorods (1D) integrated with graphene (2D) film for H_2S detection. Photoluminescence yellow emission was attributed to singly ionized oxygen vacancy in ZnO nanorods and the recombination of electron–hole pairs in graphene film. It was reported that the integrated sensor could detect H_2S (2 ppm) at room temperature [54]. The operating temperature of most of the ZnO-based sensors was found to be more than 200 ℃. As a result, the sensor would consume more power, which limits real-time application due to risky integration and the risk of gas explosion [55, 56]. To

overcome such drawbacks, copper-doped rGO/ZnO nanocomposites have been developed [57]. The morphology, response, and recovery transient of copper-doped ZnO/rGO are shown in Fig. 1.

Cu-doped ZnO nanoparticles were synthesized using a hydrothermal process, and rGO was deposited by the air-spray technique. The Cu-rGO/ZnO nanocomposites and undoped rGO/ZnO film were tested for gas-sensing properties. It was reported that Cu-doped rGO/ZnO nanocomposite exhibited high selectivity and sensitivity to H_2S at room temperature. The improved gas sensing properties of Cu-doped rGO/ZnO could be attributed to Cu and rGO both modifying Schottky barrier height and widening charge depleted region, as shown in Fig. 2.

A cost-effective, flexible, wearable gas sensor to function at room temperature is of great interest for e-textiles,

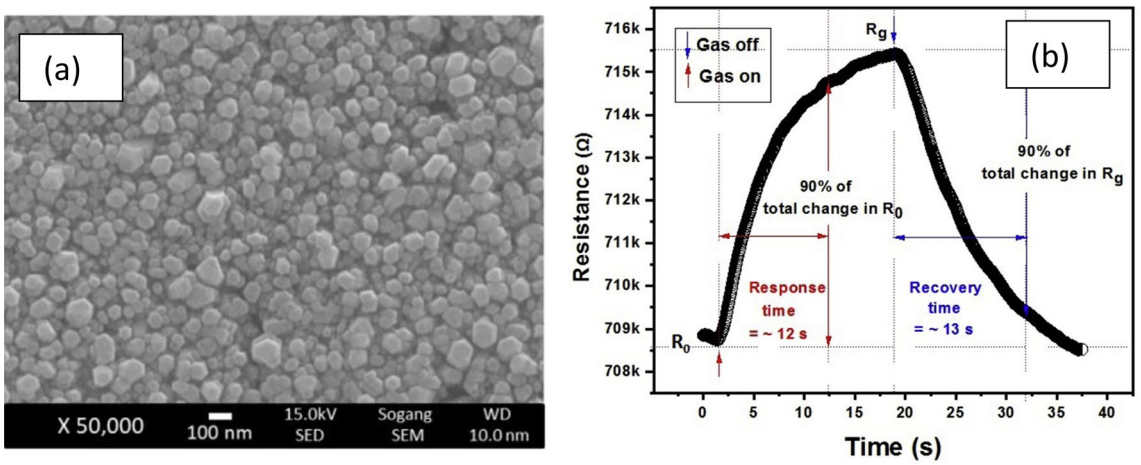

Fig. 1 FE-SEM images of **a** Cu doped ZnO/rGO and **b** Response transient plot for Cu doped ZnO/rGO nanocomposite sensor upon exposure to 150 ppm H_2S gas at 24 ℃ [57]

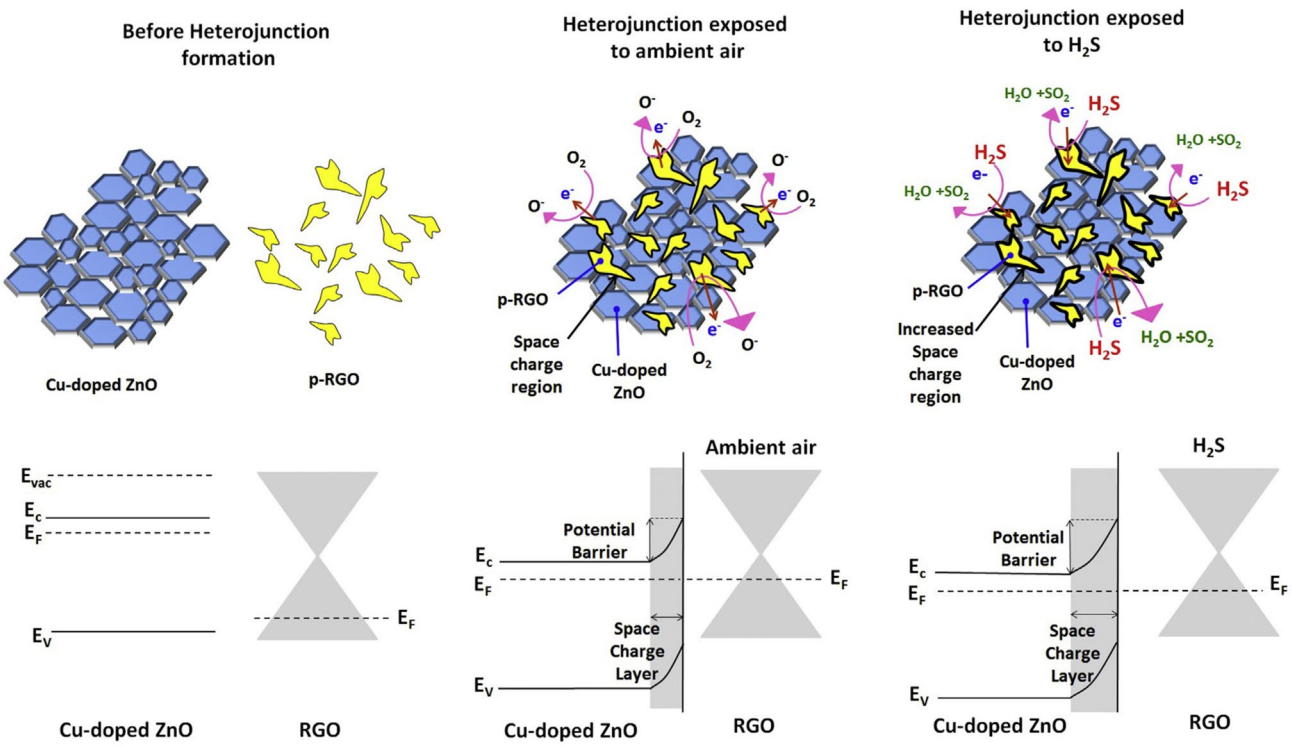

Fig. 2 Schematic illustration of the gas-sensing mechanism and band diagram illustration of the Cu-doped ZnO/RGO nanocomposite sensor [57]

the Internet of Things, and wearable electronics application. For instance, ZnO-decorated rGO fibers were developed for NO_2 and H_2S gas sensing applications [58]. It was reported that ZnO/rGO nanofibers exhibited superior gas sensing performance compared to rGO fibers alone. The enhanced sensitivity was attributed to the ZnO/rGO fibers providing more surface area for the adsorption of gas molecules and catalytic sites for gas molecules interaction. It was reported that ZnO/rGO fibers could detect H_2S 8 ppm to 100 ppm and exhibited 8 and 24-fold improved sensitivity to NO_2 and H_2S. Impedance spectroscopy is considered an effective tool for the evaluation of gas sensitivity of sensors, especially, gas sensors made of metal oxide nanohybrids. Impedance data would help to study the electrical properties of grain bulk, grain boundary, and electrode/sensing layers' interface behavior. Several research articles have been published based on impedance analysis of gas sensors made of metal oxide nanohybrids [59–67]. For instance, ZnO/rGO hybrid materials were developed for H_2S gas detection, where the gas sensitivity was evaluated using impedance spectroscopy [27]. The Nyquist plot is shown in Fig. 3b, indicating the response of the composite upon exposure to different concentrations of H_2S. Different rGO concentrations were incorporated into ZnO nano-oxide, and n-ZnO/rGO-5 exhibited better sensitivity and selectivity to H_2S. Flower-shaped ZnO nanoparticles anchored on an rGO sheet, the FESEM image of ZnO/rGO-5 nanocomposite is shown in Fig. 3a. Further, the study reported that the sensor could detect 2-100 ppm of H_2S at 90℃. Nyquist plot data revealed that the grain boundary resistance and barrier height decreased as increasing the gas concentration.

rGO/β-Ga_2O_3 composite sensor for H_2S detection

Another research paper on rGO supported β-Ga2O3 for sensitive, selective detection of H_2S, published by Sridhar et al. [68]. The authors used the impedance technique to evaluate the H_2S sensing properties of developed composites. They have reported that the sensor composed of rGO/β-Ga_2O_3 was able to detect 3 ppm of H_2S at 100℃. Impedance results revealed that grain boundary resistance of the sensing layer was highly affected by 3 ppm of H_2S compared to other common interfering gases. The authors concluded the incorporation of rGO into β-Ga_2O_3 creates an additional active surface-active site for H_2S adsorption and generates great electron transport properties; subsequently, the sensitivity and selectivity of the sensor were increased.

rGO/SnO_2 based sensor for H_2S detection

Tin oxide (SnO_2) is an n-type semiconductor with a wide gap of 3.62 eV and a wide range of industrial applications. Pristine rGO modified with SnO_2 has been developed for H_2S gas detection and reported [69]. Polyaniline (PANI) has been used for many applications as the material has electrical, optical, and chemosensitive properties to gas detection. The snO_2-based sensor is also used for human halitosis diagnosis. Halitosis is a kind of disease with a foul smell in exhaled breath. A foul smell is caused by the breakdown of food particles in the mouth, eventually releasing the foul smell. This affects health as well as social communication. This kind of halitosis could be diagnosed early with a

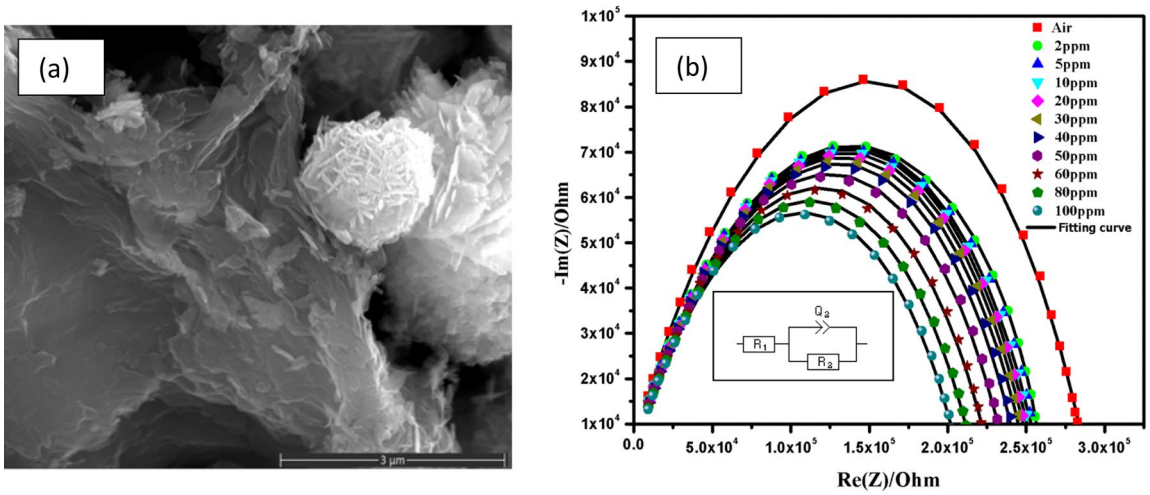

Fig. 3 FESEM image of **a** n-ZnO/rGO and **b** Nyquist impedance plot of ZnO/rGO-5 nanocomposites exposed to air and various concentrations of H_2S gas (2 – 100 ppm) at 90 °C [27]

suitable device. Dongzhi Zhang et al. developed SnO_2/rGO/PANI ternary nanocomposite to detect H_2S in exhaled breath for halitosis diagnosis in the early stage. The composite was screen printed on a flexible polyethene terephthalate substrate [70]. The sensor response towards H_2S was 23.9 for 200 ppb. The composites were characterized using FTIR, which confirmed the presence of all peaks of SnO_2, PANI, and rGO. Morphologies of SnO_2, PANI, rGO, and SnO_2/rGO/PANI samples are shown in Fig. 4. Sensor composed of SnO_2/rGO/PANI exposed to different concentrations of H_2S 50 ppb to 100 ppm and compared with SnO_2/PANI and SnO_2 (Fig. 5 a, b). It is evident that rGO incorporated SnO_2 composite shows enhanced H_2S gas sensing response compared to bare SnO_2 and SnO_2/PANI. According to this

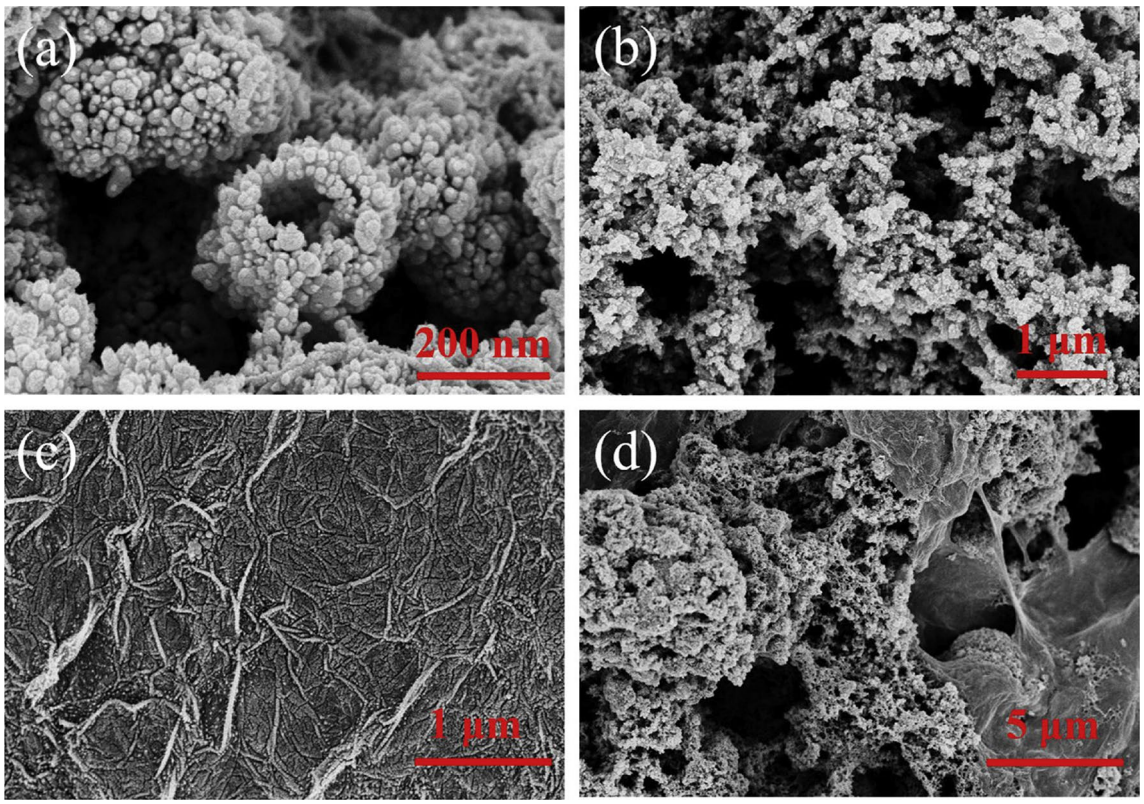

Fig. 4 SEM images of **a** SnO_2, **b** PANI, **c** rGO and **d** in-situ polymerized SnO_2/rGO/PANI composite [70]

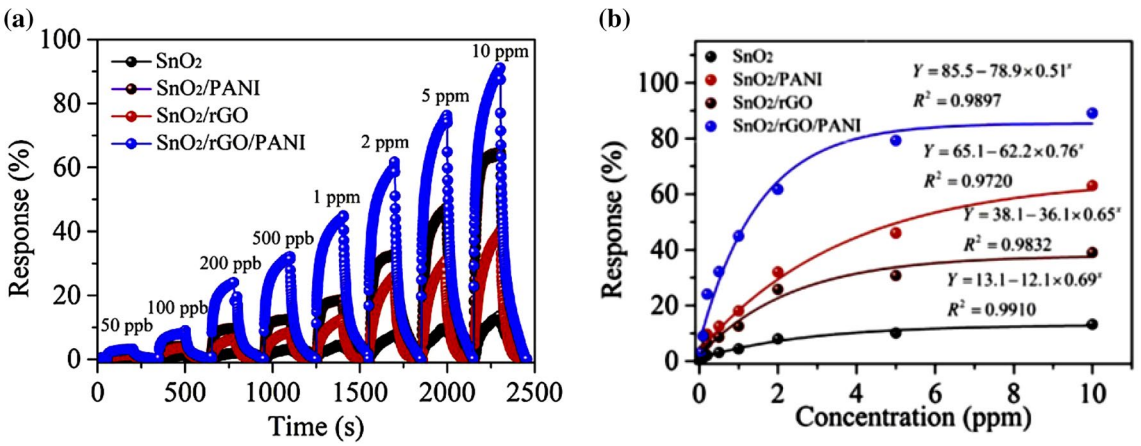

Fig. 5 **a** Response of the SnO_2, SnO_2/PANI, SnO_2/rGO, and in-situ polymerized SnO_2/rGO/PANI sensors toward H_2S. **b** Sensor response as a function of gas concentration for the SnO_2, SnO_2/PANI, SnO_2/rGO, and in-situ polymerized SnO_2/rGO/PANI sensors [70]

study, the sensor response and recovery time were 82 s and 78 s, respectively, towards 2 ppm of H_2S, which is very short compared to the SnO_2 sensor. The authors also explored the gas sensing mechanism, as shown in Fig. 6.

Figure 6a explains the mechanism of SnO_2/rGO/PANI nanocomposite toward H_2S gas as follows, the O_2^- ions are adsorbed on the sensor surface when it is exposed to atmospheric air; this causes the high resistance and thicker electron depletion layer is formed on sensing layer surface. After H_2S exposure, the resistance of the sensing layer is decreased due to the reaction between H_2S and oxygen ions on the surface. The high sensitivity was achieved due to the more surface-to-volume ratio of the composite sensor. The small hollow sphere of the composite allows the H_2S to diffuse easily, thus increasing the sensitivity. Figure 6b illustrates the inter-reaction between the p-type and n-type semiconductors to H_2S. The charge depletion layer is minimized when the sensor is exposed to the target gas, thereby decreasing the film's resistance.

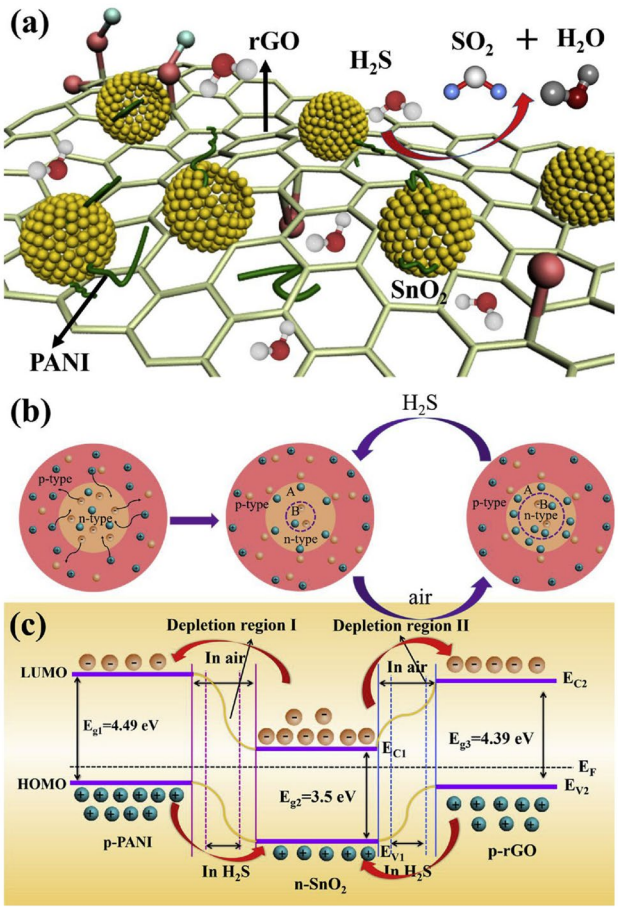

Fig. 6 **a** Mechanism diagram of the in-situ polymerized SnO_2/rGO/PANI nanocomposite toward H_2S gas. **b** Sketch of the interaction between n-type and p-type materials to H_2S. **c** p-n heterojunction in the SnO_2/rGO/PANI nanocomposite [70]

Figure 6c illustrates that the charge depletion region is formed between p-type SnO_2 and n-type rGO. When the composite sensor was exposed to H_2S gas, the electrons of rGO/PANI and holes of SnO_2 moved in the opposite direction. As a result, the thickness of the charge depletion layer decreases when the fermi energy level reaches equilibrium. Eventually, the sensor resistance decreased.

SF_6 gas has been used in gas-insulated switchgear due to its excellent insulating properties. However, SF_6 release H_2S and SO_2 when it reacts with a trace amount of H_2O and O_2 molecules. Consequently, SF_6 damage the insulation of equipment. Further, the toxicity of H_2S is well-known, and to detect decomposed products (H_2S, SO_2), rGO/SnO_2 sensor was developed and reported [71]. The rGO/SnO_2 sensor responded to 100 ppm H2S at 125 ℃. The sensor's selectivity towards H_2S and SOF_2 upon exposure to typical SF_6 decomposition components. The kinetic model and equilibrium of the rGO/SnO_2-based sensor for enhanced H_2S detection at low operating temperatures were reported [72]. Song et al. (2017) established a kinetic model to correlate sensitivity, response time, activation energy Ea and response rate constant k. Langmuir and Freundlich isotherm models were taken to fit the response curve at a different temperature, and response equilibrium parameters were extracted. According to this report, rGO-modified SnO_2 exhibited a great promoting reaction between H_2S and the surface of rGO/SnO_2 due to less activation energy (Ea—19.01 kJ mol^{-1}) than SnO_2 (Ea–20.09 kJ mol^{-1}) alone. This quantitative model would empower an exciting thought about gas sensing mechanism and enable the researchers to develop sensors operable at low temperatures for flexible electronic devices. Though the rGO/SnO_2 has exhibited great sensitivity to analyte gas, the pristine SnO_2 suffers from poor selectivity. The metal sensitizer (Pt, Pd, Au, Mn) has been incorporated into the rGO/SnO_2 matrix to improve the selectivity of the SnO_2 sensor. The selectivity of the SnO_2 sensor sensitized with the sensitizer was attributed due to the sensitizer increasing the chemisorption site, catalytic activity with the formation of Schottky barrier on the surface, and mainly interact with adsorbed oxygen molecules, thereby imparting highly selective response to target gases [59, 60, 73, 74]. For example, rGO/SnO_2 nanohybrids sensitized with Pt and Pd were developed and reported for selective detection of H_2S, NO_2, and H_2. The maximum response of 124 and 49 was obtained towards 2 and 1.6% of NO_2 and H_2, respectively. The lowest detection limits were 0.2%, 0.4, and 1 ppm for H_2, NO_2, and H_2S, respectively [75]. This study concluded that the rGO/SnO_2 nanohybrids showed excellent response kinetics to H_2S gas than NO_2 and H_2 gas.

rGO/WO_3 composite for H_2S detection

WO_3 is an n-type semiconducting material, and it has been widely used as a sensing layer for various gas (H_2, NH_3, H_2S, CH_3COCH_3, NO_2) detection due to its advantages with wide band gap energy (2.4–2.8 eV), chemical stability, electronic property, and low cost [76–82]. WO_3 has shortcomings including, poor selectivity, long response/recovery time, and poor sensitivity at low temperatures because the WO_3 has a wide band gap and high resistance at room temperature. To overcome these shortcomings, doping with other oxides and functionalization with transition metal ions were employed [83–85].

Functionalization of WO_3 with reduced graphene oxide was developed for H_2S detection [86]. The rGO/WO_3 nanosheet composite was synthesized through hydrothermal and post-calcination treatment. The composite was mixed with terpineol to form like paste and then coated on an alumina tube and annealed at 400 ℃. Morphology of (a) GO and (b) rGO/h-WO_3 composites, (c) HR-TEM image of rGO/h-WO_3 composites shown in Fig. 7. The H_2S gas sensing property of the sensor is shown in Fig. 8. The sensor response was reported to be 10.8, with a detection range of 10 ppb–40 ppm to 1 ppm of H_2S at 330 ℃. The article reported that the improved gas sensing properties were due to rGO effectively enhancing the electron's transportation/acceptance and improving the gas transportation channel in the nanostructure. The dopant materials could improve the sensing performance; however, the operating temperature was found to be still in the range of 100 ℃–400 ℃. This limits the use of WO_3 in the gas sensor for flexible and portable electronic devices.

H_2S sensor based on Fe_2O_3/graphene

Ferric oxide (Fe_2O_3) is an industrially important material as the material has a wide range of applications in the rubber industry, anti-corrosion coating, and biomedical industry [87–90]. Regardless of these applications, it was discovered that ferric oxide could detect H_2S based on chemiluminescence. Zaixing Jiang and his team reported papers like Fe_2O_3/graphene nanosheets for H_2S sensing applications

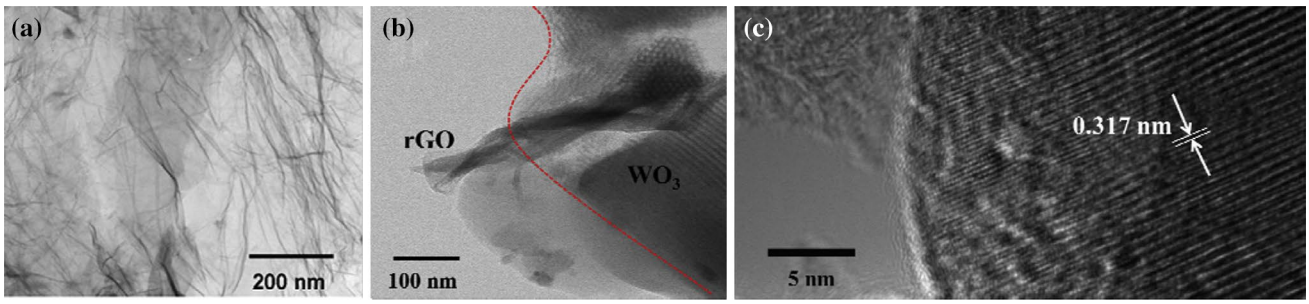

Fig. 7 TEM images of **a** GO and **b** rGO/h-WO_3composites, **c** HRTEM image of rGO/h-WO_3 composites [86]

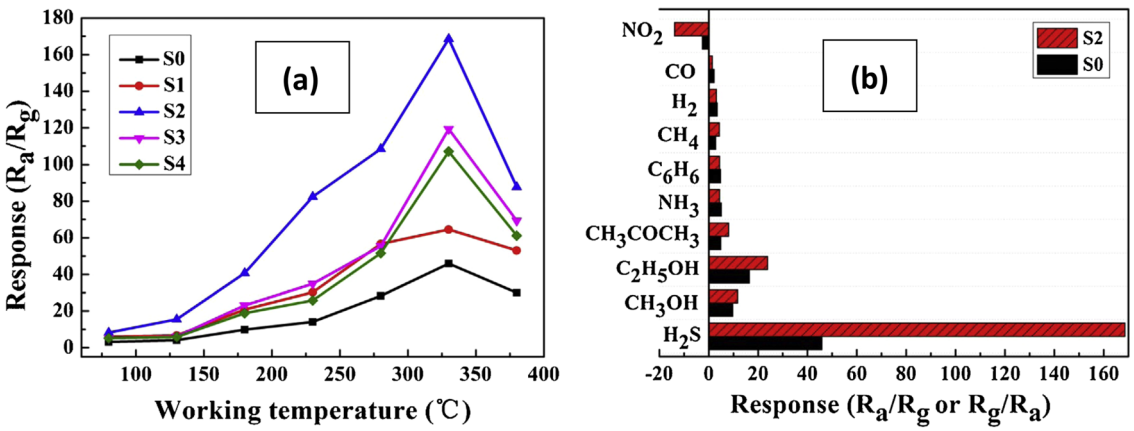

Fig. 8 H_2S gas sensing property of the sensors at different working temperatures and Responses of the sensors to various gases (the concentration of all gases was 40 ppm) [86]

[91]. The device exhibited a selective response to 10 ppm H_2S at 190 based on chemiluminescence intensity. It was reported that the Fe_2O_3/graphene paper provides a larger contact area to react with analyte gas and less resistance to flow. Enhanced gas sensing properties are generally achieved by loading the proper amount of rGO metal oxides. Nguyen Van Hoang et al. developed rGO/α-Fe_2O_3 nanofiber for enhanced H_2S sensing. The α-Fe_2O_3/rGO nanofiber was prepared by on-chip electrospinning in which optimized rGO content was loaded with a precursor solution of PVA and $Fe(NO_3)_3.9H_2O$. According to this report, the sensor response was 1.5 at 350 ℃ to 1 ppm H_2S gas, which is attributed to its porous nature, and large surface area of nanofibers loaded with 1.0 wt % of rGO. High selectivity and long-term stability were achieved due to forming a potential barrier at the heterojunction between rGO and α-Fe_2O_3. The sensor had long-term stability, i.e., 9 cycles to 1 ppm H_2S at 350 ℃. Spinel zinc ferrite is an n-type semiconducting metal oxide, in which the octahedral site was occupied by trivalent Fe^{3+}, and divalent Zn^{2+} cations occupied the tetrahedral site. Zinc ferrite has been used in lithium-ion batteries as an anode material to enhance the electrochemical properties. Recently, the material also has been utilized for H_2S gas sensing applications. Nguyen and his team developed rGO-loaded $ZnFe_2O_4$ nanofibers for H_2S detection [92].

Simple on-chip electrospinning processes were carried out to prepare rGO/$ZnFe_2O_4$ nanofibers. They reported that the rGO-loaded $ZnFe_2O_4$ nanofibers showed n-type sensing behavior, i.e., the material's resistance decreased while introducing H_2S gas. rGO/$ZnFe_2O_4$ exhibited maximum sensor response while incorporating 1.0 wt% of rGO, the response to 1 ppm of H_2S was about 147 at 350 ℃, which was 1.5 times higher than pure $ZnFe_2O_4$ nanofibers. The reported results of the selectivity and stability of the sensor are shown in Fig. 9. The highest response was attributed to heterojunction formation between rGO/ $ZnFe_2O_4$ and potential barrier at grain boundaries. Further, this study reported the 1.0 wt% of rGO-loaded $ZnFe_2O_4$ samples annealed at 600 ℃ exhibited enhanced response to 1 ppm H2S (operating temperature—350 ℃) due to the inverse effect of nanograins size and crystallinity concerning annealing temperature [93, 94].

rGO/MoO_3 based sensor for H_2S detection

Molybdenum trioxide (MoO_3) is an important n-type semiconducting material. It has been widely investigated and applied to gas sensors, catalysts, and energy storage due to its structural flexibility and polymorphism [95–97]. Recently, research on MoO_3 nanostructure for gas sensor applications has increased exponentially as it has unique properties, including high electron mobility and a high surface-to-volume ratio compared to their bulk counterparts [98–101]. However, the conductivity of MoO_3 is very low at room temperature, and it requires a high operating temperature which hinders its use in sensor applications. Research has been carried out to improve the gas sensing property of MoO_3 by doping with Fe^{2+}, in which the sensor exhibited the highest response of 184.1–100 ppm H_2S at 270 ℃ [102].

rGO has been incorporated into MoO_3 for H_2S sensing application, which still lowered the operating temperature. Bai et al. developed MoO_3 nanorods on the rGO nanosheets via the microwave hydrothermal method [103]. The sensing response of rGO/MoO_3 hybrids is presented in Fig. 10. The rGO/MoO_3 hybrids exhibited an H2S sensing response of 59 to 40 ppm H_2S at 110 ℃, and the response and recovery were found to be 9 s and 17 s, respectively. MalekAlaie et al. prepared MoO_3 decorated with rGO and studied H_2S gas sensing properties. The sensor was fabricated by spin coating rGO/MoO_3 on an alumina substrate. The highest response was obtained at 160 ℃ for the 3wt% MoO_3–rGO

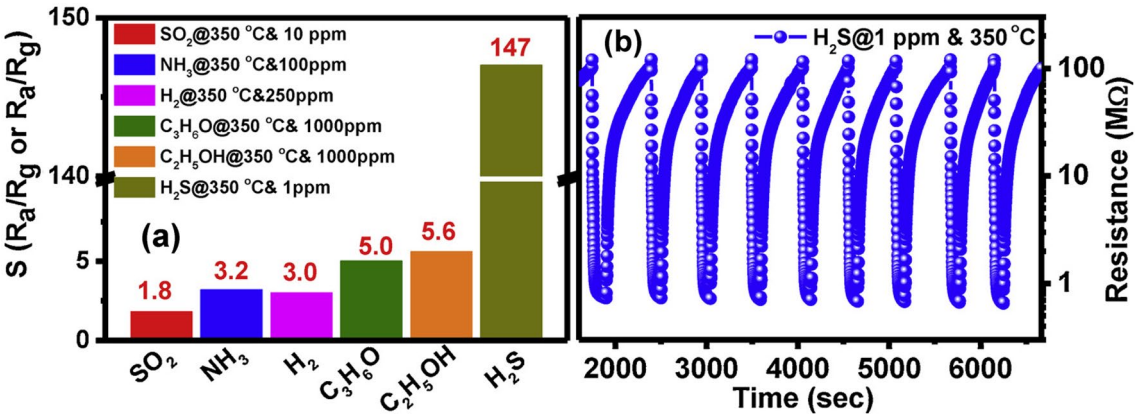

Fig. 9 Selectivity to various gases at 350 °C **a** and stability at 1 ppm H_2S gas at 350 °C **b** of the sensors based on the 1 wt.% RGO-loaded $ZnFe_2O_4$ NFs calcined at 600 °C [87]

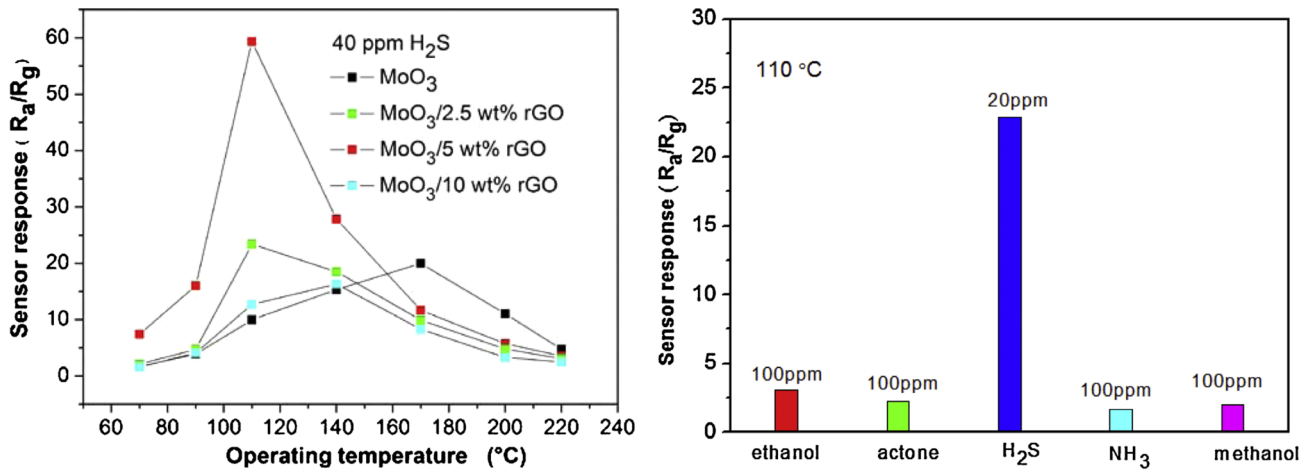

Fig. 10 Sensing responses of MoO_3/rGO hybrids with different graphene content to 40 ppm H_2S and Response of -MoO_3/5 wt% rGO hybrid-based sensor to different gases [103]

and was highly selective to H_2S gas than common interfering gases [104].

rGO/CuO based sensor for H_2S detection

Copper oxide (CuO) is a p-type semiconducting oxide, having a band gap energy of 1.35 eV. Most often, it has been incorporated with other n-type semiconducting metal oxides for H_2S gas sensing studies [82, 105]. It is well known that CuO is converted into metallic CuS when in contact with H_2S gas even under ambient conditions. However, the desulfuration of CuO is poor at room temperature and it requires a high operating temperature. CuO combined with n-type material, forming heterostructure at the interface, can modulate carrier transport channel, and facilitate decomposition of analyte gas molecules. CuO nanoparticles combined with rGO have been prepared via a microwave-assisted method and studied for H_2S gas sensing properties [106]. The obtained CuO@rGO composite was dispersed in aqueous/water for sensor measurement and dropped on interdigitated Au electrode to form a resistive film. The response profile of the sensor exposed to H_2S gas is presented in Fig. 11.

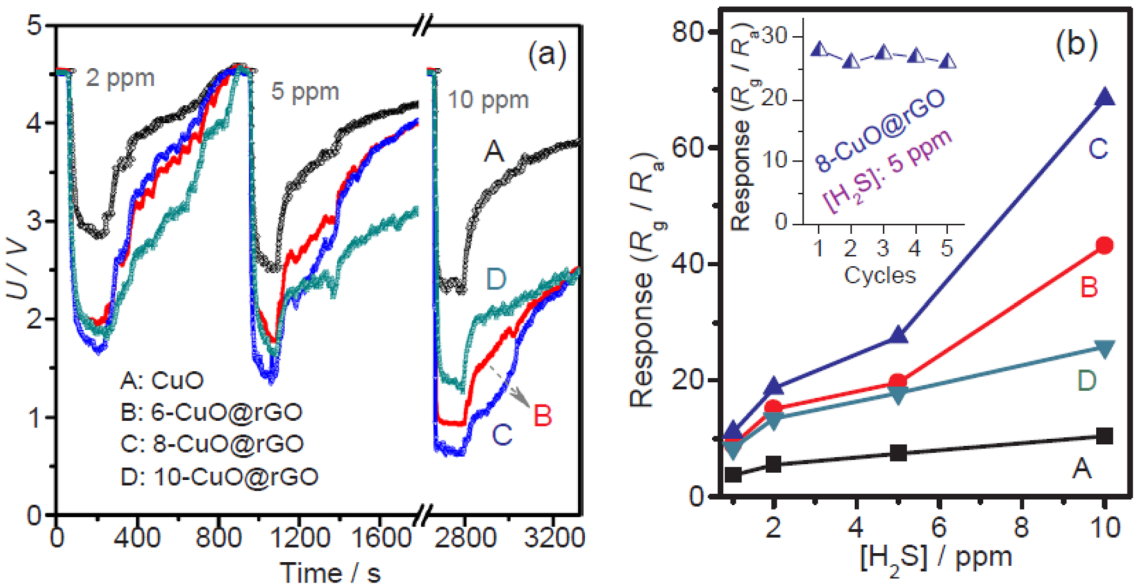

Fig. 11 **a** Response profiles to H_2S gases and **b** plots of the response versus [H_2S] operating at 100 °C: (A) CuO, (B) 6-CuO@rGO, (C) 8-CuO@rGO, and (D) 10-CuO@rGO. The insert is the repeated response of the 8-CuO@rGO sensor to H_2S gas at 100 °C [106]

The authors demonstrated the gas sensing mechanism of the sensor exposed to H_2S gas in Fig. 12. According to this study, the composite composed of rGO/CuO is a p-type semiconductor with holes as the main carrier [107]. Adsorbed oxide ions (O^-, O^{2-}, O_2^-) are generated on rGO/CuO surfaces in ambient air. Thus, less resistance is formed on the surface. The conductivity is increased when the sensor is exposed to H_2S by reacting with oxide ions (Fig. 12).

Research on Cu_2O has been explored for gas sensor application, but the gas sensitivity is limited, and the operating temperature was typical > 150 ℃ , as closely packed Cu_2O on interdigitated electrode (IDE) allows low electrons to flow. Sensor working at high temperature does give high sensing property, but it is difficult during device (inbuilt with heater) fabrication and explosive risks. Functionalization with graphene could realize the sensor operable at room temperature. Lisha Zhou et al. developed Cu_2O/graphene sheets for enhanced H_2S sensing properties. Au/Cr IDE was prepared through photolithography and sputtering. Cu_2O/Graphene was drop cast on IDE and dried to evaporate the solvent. I-V characteristics showed that the Cu_2O conductivity was poor and higher for Cu_2O/Graphene composite. The composite exhibited Schottky contacts rather than ohmic behavior as the composite covered uniformly on the IDE substrate. The resistance of the composite was increased with increasing H_2S gas concentration (5 ppb to 100 ppb) at room temperature. It was reported the high sensitivity was attributed to the nano-size effect and interfacial bonding between graphene and Cu_2O.

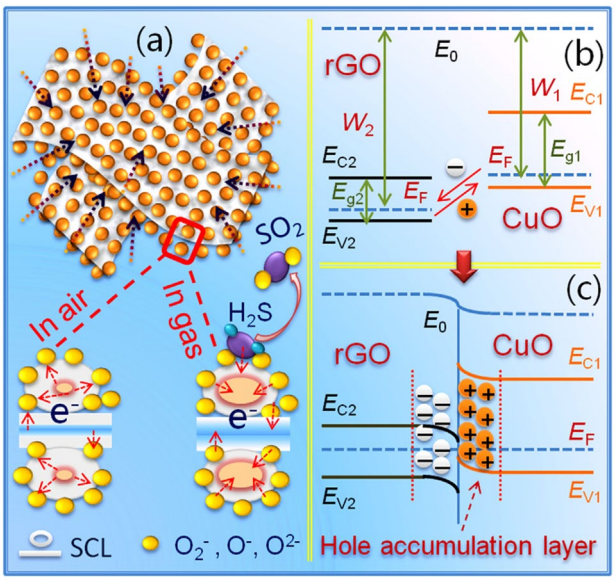

Fig. 12 A schematic demonstration of the CuO@rGO sensor to H_2S gas: **a** the adsorption and reaction process and **b**, **c** the qualitative evolution diagram of the two energy bands [106]

CuO is transformed to CuS when injecting H_2S, the desulfuration can be as follows

$$CuO(s) + H_2S(g) \rightarrow CuS(s) + H_2O(g)$$

$$CuS(s) + {}^3/_2O_2(g) \rightarrow CuO(s) + SO_2(g)$$

It was reported that the work function for CuO and CuS is as follows 3.61 eV and 4.9 eV, respectively [107]. Due to this work function difference, the electrons flow from CuO to CuS at the CuO/CuS heterointerfaces, establishing a potential barrier. The potential barrier will be minimized when the grain boundary region is converted to CuS. The CuS conversion back to CuO is achieved during the recovery period.

H_2S sensing characteristics of various rGO/MOx-based sensor is provided in Table 1.

H_2S sensor based on Carbon nanotube/ Metal oxide composites

The principal requirement for the highly sensitive gas sensor is the structure must be a high surface-to-volume ratio. Porous thick and thin film structures have been designed to obtain highly sensitive sensors. Carbon nanotube (CNT) is a class of advanced materials having a wide range of applications due to their excellent physicochemical properties. It is generally categorized into two types: conducting and semiconducting nanotubes. Further, these CNT can be either single-walled or multi-walled nanotubes. Carbon nanotubes are highly reactive gaseous molecules adsorbed on the surface by charge conversion at RT. Nathan et al. reported CNT-modified electrodes for H_2S detection using an electrochemical method [110]. It was reported the electrode had a low potential response towards H_2S. Glassy carbon-modified electrodes had a linear range of 1.25–112.5 µM with a detection limit of 0.3 µM (9 ppb). Further, it was reported the electrode was more stable and selective to sulfide, enabling the development of a sensor for real-time application. Jun Fan et al. developed CuO/SnO_2 doped with acidified CNT to detect H_2S at low concentrations [111]. It was reported the developed sensor exhibited excellent sensitivity to H_2S ranging from 0.1 to 0.5 ppm at 40℃, and response and recovery time was found to be 8.3 s and 11.5 s, respectively. The formation of p-n heterojunction between CuO/SnO_2 and CNT introduced nanochannel and played a major role. Hyun Young Jung et al. reported highly effective detection of H_2S by CNT functionalized with 2,2,6,6–tetramethylpiperidine- 1- oxyl (TEMPO). The device exhibited high H_2S sensitivity of 420% at 60% humidity. Navaratnarajah and his co-worker reported Ru-doped SWCNT for H_2S and SO2 detection [112]. Spin-polarized DFT simulations were used

Table 1 H_2S gas sensing characteristics of sensors based on rGO/MOx

Sensing material	Fabrication method	Operating temperature, ℃	Response (%)	Response time,	Recovery time,	Lowest detection limit	References
rGO/CuO	Electrospinning	300	11.7 (10 ppm)	–	–	1 ppm	[108]
SnO_2/rGO/PANI	in-situ polymerization technique	Room temperature	9.1 (0.1 ppm)	82 s	78 s	50 ppb	[70]
SnO_2/RGO: Pt	Hydrothermal	200	3.7 (40 ppm)	–	–	1 ppm	[75]
rGO/SnO_2	Solvothermal	70	40 (10 ppm)	–	–	5 ppm	[72]
rGO/WO_3	Hydrothermal	330	168.58 (40 ppm)	7 s	55 s	10 ppb	[86]
rGO/MoO_3	Wet chemical	160	4120 (50 ppm)	60 s	120 s	50 ppm	[104]
rGO/CuO	Microwave assisted in-situ growth	100	68.5 (10 ppm)	20 s	920 s	1 ppm	[106]
rGO/ZnO	Electrospun on onto microelectrode chip	350	1353 (1 ppm)	10 s	The 1520 s	1 ppm	[50]
Cu- ZnO/RGO	Hydrothermal, and Air spray coating	24	0.87 (100 ppm)	14 s	32 s	4 ppm	[57]
rGO/ZnO	Hydrothermal-assisted chemical reduction	Room temperature	2.68 (20 ppm)	404 s	275 s	8 ppm	[58]
rGO/ZnO	One-step solution synthesis	90	–	–	–	2 ppm	[27]
rGO/ZnO	Hydrothermal	160	55.91(50 ppm)	35 s	410 s	1 ppm	[49]
Graphene/ZnO	Solution Process	Room temperature	–	–	–	2 ppm	[54]
rGO/SnO_2	One-step hydrothermal	125	33.02 (100 ppm)	209 s	900 s	1 ppm	[71]
rGO/Fe_2O_3	On-chip electrospinning	350	9.2 (1 ppm)	–	–	0.1 ppm	[109]
rGO/$ZnFe_2O_4$	On-chip electrospinning	350	147 (1 ppm)	–	–	0.1 ppm	[92]
rGO/MoO_3	In-situ one-step microwave hydrothermal method	110	59 (40 ppm)	9 s	17 s	5 ppm	[103]

to determine the encapsulation and adsorption behavior of H_2S and SO_2 gas molecules by Ru-doped CNT. Ru doping on CNT slightly enhanced the adsorption efficacy. However, the obtained results should be confirmed by practical experiments. H_2S sensing characteristics of various rGO/MOx-based sensor is provided in Table 2.

Asad et al. developed copper-decorated SWCNT for highly sensitive and selective detection of H_2S [118]. Copper-decorated SWCNT was prepared by the chemical reduction process. The sample was spin-coated on Al patterned flexible substrate and annealed in a vacuum oven at 80 °C for 30 min. The sensor response/recovery was reported to be ~ 10 s and ~ 15 s, respectively, to 5 ppm H_2S gas.

Mohsen Asad et al. reported hybrid nanomaterials based on CuO/SWCNT for wireless H_2S sensing applications [121]. CuO with different morphologies was synthesized by hydrothermal method, and SWCNT was functionalized by mixing 20 mg into CuO, stirred at 100 ℃ for 30 min. As a prepared sample, CuO/SWCNT was spin-coated on Au IDE structured electrode to obtain a thin film for gas sensing studies. The study summarized that a fabricated wireless sensor could detect 100 ppb H_2S gas. The SWCNT formed as an effective charge carrier channel also reported that it caused quick response 7 s to 1 ppm H_2S. The reported gas-sensing mechanism of the sensor is presented in Fig. 13. It was reported the sensing mechanism (Fig. 13) of CuO-SWCNT gas sensors to H_2S follows, at ambient air, oxygen adsorbed on CuO surface forming as $3O_2^-$ by extracting electron from CuO conduction band. When H_2S gas molecules interact with oxygen ions, the trapped electrons are released and go towards CNTs due to the high electron affinity of the SWCNTs, as results decrease in the conductivity of p-type SWCNTs. At higher concentrations of gas, in addition to H_2S oxidation, a chemical reaction between H_2S and CuO causes the formation of the CuS layer (inset Figure Eq. 2).

Soyeon Moon et al. developed the Co_3O_4-SWCNT composite by arc discharge method for H_2S detection [117]. The sensor structure was fabricated on an alumina substrate patterned with a gold electrode. The porous nature of the composite was observed through Sem and XRD analysis. The response profile of the sensor is shown in Fig. 14. For gas sensing studies, Co30–SWCNT composite film

Table 2 H_2S sensing characteristics of various CNT/MOx-based sensor

Sensing material	Fabrication method	Operating temperature, ℃	Response (%)	Response time,	Recovery time,	Lowest detection limit	References
CNTs-CuO/SnO_2	Co-dissolution and electrospinning	40	4.441	8.3 s	11.5 s	0.1 ppm	[111]
CNTs/SnO_2/CuO	Sol–Gel	Room temperature	4.41	4 min	10 min	10 ppm	[113]
MWCNTs-COOH	MWCNTs-COOH deposited on PTFE membrane	Room temperature	–	6.06 min	4.13 min	310 ppb	[114]
MWCNTs-CuO/Cu_2O	MWCNTs sprayed on an alumina substrate, Cu sputtered on substrates that were spray-coated with MWCNTs	150	1244	219 s	77 s	1 ppm	[115]
SWNT-COOH	Chemical vapor deposition	Room temperature	0.986	6–8 min	10 min	20 ppb	[116]
Co_3O_4–SWCNT	Arc discharge method	250	500	–	–	5 ppm	[117]
Cu-SWCNT	Chemical reduction process, Spin coating	Room temperature	25	10 s	20 s	5 ppm	[118]
$NiFe_2O_4$–MWCNTs	Sol–gel, Spin coating	300	250	110 s	2 min	100 ppm	[119]
Cu -SWCNT	Chemical reduction, Drop casting	175	90	7 s	9 s	5 ppm	[120]
CuO-SWCNT	Hydrothermal, Drop casting	Room temperature	–	7 s	28 s	100 ppb	[121]
SWCNT-TEMPO	Dip coating	Room temperature	420	–	–	10 ppm	[122]

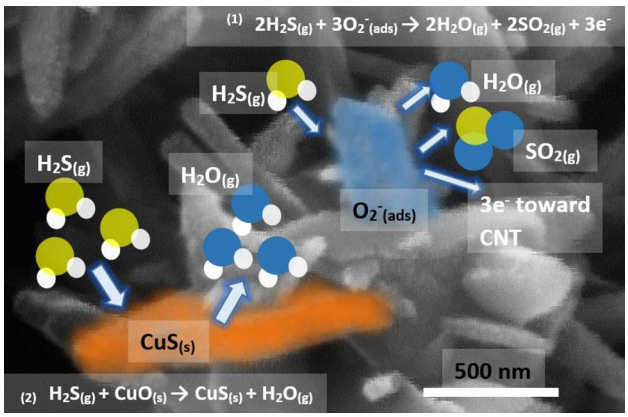

Fig. 13 Schematic of the sensing mechanism of fabricated CuO-SWCNT gas sensors were exposed to H_2S. [121]

exhibited the highest response to 100 ppm H_2S at 250℃. The composite film resistance decreased when exposed to H_2S (5–150 ppm), indicating the film behaved p-type semiconductor. Thus, the CNT in the film played a transport path and had not contributed to gas sensing. Functionalizing CNT with some chemical reactants could improve conductivity and compensate for drawbacks like less response and lack of sensitivity. To improve the CNT sensor performance, functionalized multiwall carbon nanotube (MWCNTs-COOH) has been prepared and evaluated for H_2S sensing performance. For example, Nosrat Izadi et al. investigated the effect of functionalized MWCNTs on H_2S sensing properties. The carbon nanotubes were synthesized by chemical vapor deposition and functionalized with carboxyl, amide groups, Pt, and Mo nanoparticles. Mo/CNT and Pt/CNT-COOH-based sensors exhibited the highest response than CNT-COOH-based sensors. The highest response is attributed to discrete band gap states induced by metallic nanoclusters on the CNT surface, generating additional charge transfer between CNT and gas molecules to enhance gas sensitivity. Carboxylated MWCNTs were developed and used as counter and working electrodes while H_2S sensing [114]. Oxidation of H_2S on the working electrode produces a current which is directly proportional to gas concentration depending on the electrode characteristics. Cyclic voltammetry with a scan rate of 0.1 V/s was conducted for MWCNT and carboxylated MWCNT electrodes to examine the H_2S (500 ppm) sensitivity before and after exposure. It was concluded the carboxylated MWCNT exhibited a slightly higher response than raw MWCNT. To improve the sensing characteristics of MWCNT, Jae Hoon Bang et al. developed MWCNT decorated CuO/Cu_2O nanoparticles for selective sensing of H_2S and reported [115].

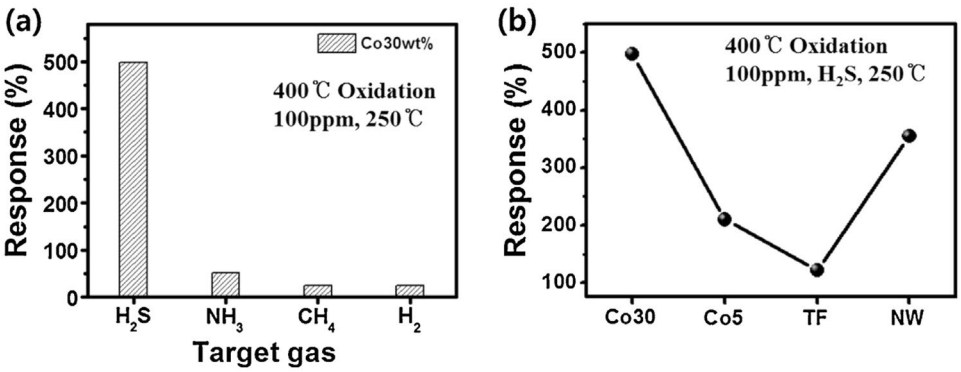

Fig. 14 **a** The gas selectivity of the Co30-400 sensor to H_2S was derived from a comparison with the responses to typical reducing gases of NH_3, CH_4, and H_2. **b** Comparison of sensing responses of Co30-400 and Co5-400 with sensors of thin film Co_3O_4 and nanowires of Co_3O_4–SWCNT [117]

A different layer of Cu was sputtered on MWCNT and annealed at 500 ℃. The developed MWCNT decorated CuO/Cu_2O formed a p-p heterojunction. According to their study, the sensor response was 1244% to 1 ppm H_2S, and response and recovery time was 219 s and 77 s, respectively. Decorating carbon nanotubes with Mn, Co, Mg, and Zn can improve magnetic, optical, and electrochemical properties, consequently enhancing the H_2S gas sensitivity. Hajihashemi et al. synthesized $NiFe_2O_4$–MWCNT by sol–gel method and reported the H_2S gas sensing behavior of the prepared material. It was reported that crystallite size of the composite material found to be 23.93 nm. The sensing film was prepared by spin coating method and exhibited appropriate response to 100 ppm of H_2S gas. Superior sensitivity was achieved due to incorporation of carbon nanotube which act as substrate and transferred temperature to $NiFe_2O_4$. Further, surface morphology and surface-to-volume ratio of the composite play a role in adsorption of more H_2S on the surface of materials [119].

Conclusions and future perspectives

In this article, we critically reviewed a significant achievement in the field of H_2S sensors made of carbonaceous materials and doped metal oxides. The general approach to enhancing the H_2S sensing behavior of the MOx sensor is to incorporate optimized carbonaceous materials (CNT, graphene, and rGO). Incorporating those carbonaceous materials enhances gas sensitivity, decreasing the sensor operating temperature and reducing sensor response time, leading to composites contending the sensor made of metal oxides alone. For over a decade, extensive research has been conducted based on rGO/MOx for H_2S detection. However, the H_2S detection based on carbonaceous materials reported in this article is basic research and needs a lot of investigation such as sensor behavior at different humidity, temperature, etc., are required to build a sensor for monitoring H_2S to be deployable in the field, and indeed the researchers are working extensively to develop that type of sensor. Most research articles explain the sensing mechanism but need to explain the chemical nature of sensing materials and the selectivity mechanism. In future work on developing an H_2S gas sensor-based carbonaceous material for real-time monitoring, one should note that the sensor performance is based on humidity, temperature, and interfering gases. The selectivity of carbonaceous/metal oxide-based sensors could be achieved by the functionalization of new molecules which are specifically interacting with the target gas. The effect on humidity could be stabilized by coating with appropriate hydrophobic materials. The carbonaceous materials (CNT, graphene, rGO)/MOx-based sensors still need to be evaluated under different volatile organic compounds.

Data availability The datasets supporting the conclusions of this article are included within the article.

Declarations

Conflict of interest The authors are declaring that there is no conflict of interest.

References

1. K. Vikrant, V. Kumar, Y.S. Ok, K.-H. Kim, A. Deep, Metal-organic framework (MOF)-based advanced sensing platforms for the detection of hydrogen sulfide. TrAC, Trends Anal. Chem. **105**, 263–281 (2018)
2. A. Mirzaei, S.S. Kim, H.W. Kim, Resistance-based H_2S gas sensors using metal oxide nanostructures: a review of recent advances. J. Hazard Mater. **357**, 314–331 (2018)
3. K.S. Yoo, S.D. Han, H.G. Moon, S.-J. Yoon, C.-Y. Kang, Highly sensitive H_2S sensor based on the metal-catalyzed SnO_2 nanocolumns fabricated by glancing angle deposition. Sensors **15**, 15468–15477 (2015)
4. C.S. Rout, M. Hegde, C.N.R. Rao, H2S sensors based on tungsten oxide nanostructures. Sens. Actuators B Chem. **128**, 488–493 (2008)
5. S. Navale et al., CuxO nanostructure-based gas sensors for H_2S detection: an overview. Chemosensors **9**(6), 127 (2021)
6. V. Vitvitsky, R. Banerjee, Chapter Seven - H_2S analysis in biological samples using gas chromatography with sulfur chemiluminescence detection. in methods in enzymology (eds. Cadenas, E. & Packer, L.) vol. 554 p. 111–123 (Academic Press, 2015).

7. H. Ibrahim, A. Serag, M.A. Farag, Emerging analytical tools for the detection of the third gasotransmitter H_2S, a comprehensive review. J Adv Res **27**, 137–153 (2021)
8. A. Mirzaei, S.G. Leonardi, G. Neri, Detection of hazardous volatile organic compounds (VOCs) by metal oxide nanostructures-based gas sensors: a review. Ceram Int **42**, 15119–15141 (2016)
9. P.J. Sabourin, W.E. Bechtold, R.F. Henderson, A high pressure liquid chromatographic method for the separation and quantitation of water-soluble radiolabeled benzene metabolites. Anal. Biochem. **170**, 316–327 (1988)
10. G. Sarala Devi, S. Manorama, V.J. Rao, High sensitivity and selectivity of an SnO_2 sensor to H_2S at around 100 °C. Sens. Actuators B Chem. **28**, 31–37 (1995)
11. S.D. Shinde, G.E. Patil, D.D. Kajale, V.B. Gaikwad, G.H. Jain, Synthesis of ZnO nanorods by spray pyrolysis for H_2S gas sensor. J. Alloys Compd. **528**, 109–114 (2012)
12. D. Li et al., Ultra-highly sensitive and selective H_2S gas sensor based on CuO with sub-ppb detection limit. Int J Hydrogen Energy **44**, 3985–3992 (2019)
13. H.-M. Lin, C.-M. Hsu, H.-Y. Yang, P.-Y. Lee, C.-C. Yang, Nanocrystalline WO_3-based H_2S sensors. Sens. Actuators B Chem. **22**, 63–68 (1994)
14. L. Zhang et al., Self-assembly gridding α-MoO_3 nanobelts for highly toxic H_2S gas sensors. Sens Actuators B Chem **237**, 350–357 (2016)
15. J. Xu, X. Wang, J. Shen, Hydrothermal synthesis of In_2O_3 for detecting H_2S in air. Sens. Actuators B Chem. **115**, 642–646 (2006)
16. Z. Li et al., A fast response & recovery H_2S gas sensor based on α-Fe_2O_3 nanoparticles with ppb level detection limit. J. Hazard Mater. **300**, 167–174 (2015)
17. Akhtar, F. S. E.-S. B. K. E.-A. M. A. E.-K. 2019 Metal Oxide Gas Sensors by Nanostructures. in Gas Sensors Ch. 1 (IntechOpen). https://doi.org/10.5772/intechopen.88858
18. N. Tao, Challenges and promises of metal oxide nanosensors. ACS Sens. **4**, 780 (2019)
19. C. Su et al., Controllable synthesis of heterostructured CuO–NiO nanotubes and their synergistic effect for glycol gas sensing. Sens. Actuators B Chem. **304**, 127347 (2020)
20. Z. Yang et al., Construction, application and verification of a novel formaldehyde gas sensor system based on Ni-doped SnO_2 nanoparticles. IEEE Sens J **21**, 11023–11030 (2021)
21. X. Chen et al., Two-dimensional Cd-doped porous Co_3O_4 nanosheets for enhanced room-temperature NO_2 sensing performance. Sens. Actuators B Chem. **305**, 127393 (2020)
22. L. Xu et al., A novel CoxNi1-xP/fs-Si self-supporting electrodes manufactured via femtosecond laser for highly efficient hydrogen evolution reaction. Surf. Interfaces **32**, 102173 (2022)
23. C. Yang et al., Indium element - induced oxygen vacancies and polycrystalline structure enabled SnO_2 nanofibers for highly sensitive detection of NOx. Sens. Actuators B Chem. **362**, 131754 (2022)
24. C. Yang et al., High selectivity of Ag-doped Fe_2O_3 hollow nanofibers in H_2S detection at room operating temperature. Sens. Actuators B Chem. **341**, 129919 (2021)
25. C. Zhang, S. Zhang, Y. Yang, H. Yu, X. Dong, Highly sensitive H_2S sensors based on metal-organic framework driven γ-Fe_2O_3 on reduced graphene oxide composites at room temperature. Sens. Actuators B Chem. **325**, 128804 (2020)
26. S. Zhang et al., Femtosecond laser micro-nano processing for boosting bubble releasing of gas evolution reactions. Nano. Res. **15**, 1672–1679 (2022)
27. V. Balasubramani, S. Sureshkumar, T.S. Rao, T.M. Sridhar, Impedance spectroscopy-based reduced graphene oxide-incorporated ZnO composite sensor for H_2S investigations. ACS Omega **4**, 9976–9982 (2019)
28. S. Mallakpour, E. Khadem, Carbon nanotube–metal oxide nanocomposites: fabrication, properties and applications. Chem. Eng. J. **302**, 344–367 (2016)
29. R. Leghrib, A. Felten, J.J. Pireaux, E. Llobet, Gas sensors based on doped-CNT/SnO_2 composites for NO_2 detection at room temperature. Thin Sol. Films **520**, 966–970 (2011)
30. D. Jung, M. Han, G.S. Lee, Room-temperature gas sensor using carbon nanotube with cobalt oxides. Sens. Actuators B Chem. **204**, 596–601 (2014)
31. H. Liu et al., Synthesis and gas sensing characteristic based on metal oxide modification multi wall carbon nanotube composites. Appl. Surf. Sci. **258**, 1991–1994 (2012)
32. A. Wisitsoraat, A. Tuantranont, C. Thanachayanont, V. Patthanasettakul, P. Singjai, Electron beam evaporated carbon nanotube dispersed SnO_2 thin film gas sensor. J. Electroceram. **17**, 45–49 (2006)
33. D. Punetha, S.K. Pandey, Sensitivity enhancement of ammonia gas sensor based on hydrothermally synthesized rGO/WO_3 nanocomposites. IEEE Sens. J. **20**, 1738–1745 (2020)
34. D. Guo et al., Reduced-graphene-oxide/metal-oxide p-n heterojunction aerogels as efficient 3D sensing frameworks for phenol detection. Carbon N Y **99**, 571–578 (2016)
35. V.S. Bhati et al., Improved sensitivity with low limit of detection of a hydrogen gas sensor based on rGO-loaded Ni-doped ZnO nanostructures. ACS Appl. Mater. Interfaces **10**, 11116–11124 (2018)
36. P.-G. Su, L.-Y. Yang, NH_3 gas sensor based on Pd/SnO_2/RGO ternary composite operated at room-temperature. Sens. Actuators B Chem. **223**, 202–208 (2016)
37. Z. Yuan, Y. Liu, J. Zhang, F. Meng, H. Zhang, Rose-like MoO_3/MoS_2/rGO low-temperature ammonia sensors based on multigas detection methods. IEEE Trans. Instrum. Meas. **70**, 1–9 (2021)
38. X. Li et al., Reduced graphene oxide (rGO) decorated TiO_2 microspheres for selective room-temperature gas sensors. Sens. Actuators B Chem. **230**, 330–336 (2016)
39. T. Salehi, A. Taherizadeh, A. Bahrami, A. Allafchian, V. Ghafarinia, Toward a highly functional hybrid ZnO nanofiber–rGO gas sensor. Adv. Eng. Mater. **22**, 2000005 (2020)
40. O. Ogbeide et al., Inkjet-printed rGO/binary metal oxide sensor for predictive gas sensing in a mixed environment. Adv Funct Mater n/a **32**(25), 2113348 (2022)
41. P. Hao, Z. Lin, P. Song, Z. Yang, Q. Wang, rGO-wrapped porous $LaFeO_3$ microspheres for high-performance triethylamine gas sensors. Ceram Int **46**, 9363–9369 (2020)
42. S. Moon et al., Co_3O_4-SWCNT composites for H_2S gas sensor application. Sens. Actuators B Chem. **222**, 166–172 (2015)
43. S. Sureshkumar, B. Venkatachalapathy, T.M. Sridhar, Enhanced Hsub2/subS gas sensing properties of Mn doped ZnO nanoparticlesan impedance spectroscopic investigation. Mater. Res. Express **6**, 75009 (2019)
44. S. Sureshkumar, B. Jothimani, T.M. Sridhar, A. Santhosh, B. Venkatachalapathy, Synthesis of hexagonal ZnO-PQ7 nano disks conjugated with folic acid to image MCF – 7 cancer cells. J. Fluoresc. **27**, 21–29 (2017)
45. S. Lakshmipurada, K. Reddy, S. Sundaravel, Synthesis and characterization of activated carbon/ZnO nanocomposite from water hyacinth for heavy metals adsorption and its antimicrobial activity. Asian J. Chem. **33**, 551–556 (2021)
46. D. Li et al., Preparation and gas-sensing performances of ZnO/CuO rough nanotubular arrays for low-working temperature H_2S detection. Sens. Actuators B Chem. **254**, 834–841 (2018)
47. H. Wang, Y. Luo, B. Liu, L. Gao, G. Duan, CuO nanoparticle loaded ZnO hierarchical heterostructure to boost H_2S sensing with fast recovery. Sens. Actuators B Chem. **338**, 129806 (2021)

48. S. Park et al., Enhanced H_2S gas sensing performance of networked CuO-ZnO composite nanoparticle sensor. Mater. Res. Bull **82**, 130–135 (2016)
49. Y. Shen et al., Preparation and sensing properties of mesoporous ZnO–rGO composites based on in situ hydrothermal synthesis. J. Mater. Sci.: Mater. Electron. **27**, 12660–12668 (2016)
50. T.K. Dang et al., Extraordinary H_2S gas sensing performance of ZnO/rGO external and internal heterojunctions. J Alloys Compd **879**, 160457 (2021)
51. S. Singkammo et al., Electrolytically exfoliated graphene-loaded flame-made Ni-doped SnO_2 composite film for acetone sensing. ACS Appl. Mater. Interfaces **7**, 3077–3092 (2015)
52. D. Fu, C. Zhu, X. Zhang, C. Li, Y. Chen, Two-dimensional net-like SnO2/ZnO heteronanostructures for high-performance H_2S gas sensor. J. Mater. Chem. A Mater. **4**, 1390–1398 (2016)
53. F.-L. Meng, Z. Guo, X.-J. Huang, Graphene-based hybrids for chemiresistive gas sensors. TrAC, Trends Anal. Chem. **68**, 37–47 (2015)
54. T.V. Cuong et al., Solution-processed ZnO-chemically converted graphene gas sensor. Mater Lett **64**, 2479–2482 (2010)
55. Z. Li et al., Advances in designs and mechanisms of semiconducting metal oxide nanostructures for high-precision gas sensors operated at room temperature. Mater. Horiz. **6**, 470–506 (2019)
56. D. Sun, Y. Luo, M. Debliquy, C. Zhang, Graphene-enhanced metal oxide gas sensors at room temperature: a review. Beilstein J. Nanotechnol. **9**, 2832–2844 (2018)
57. P.S. Shewale, K.S. Yun, Synthesis and characterization of Cu-doped ZnO/RGO nanocomposites for room-temperature H_2S gas sensor. J Alloys Compd **837**, 155527 (2020)
58. A.D. Ugale et al., ZnO decorated flexible and strong graphene fibers for sensing NO2 and H_2S at room temperature. Sens. Actuators B Chem. **308**, 127690 (2020)
59. S.S. Kumar, B. Venkatachalapathy, L. Sujatha, T.S. Rao, T.M. Sridhar, Influence of H_2S concentration on Mn sensitized tin dioxide nanoparticles based sensor—an impedance spectroscopic investigation. Sens. Lett. **14**, 949–954 (2016)
60. S. Sureshkumar, B. Venkatachalapathy, T.M. Sridhar, Enhanced H_2S gas sensing properties of Mn doped ZnO nanoparticles—an impedance spectroscopic investigation. Mater Res Express **6**(7), 075009 (2019)
61. F. Schipani et al., Electrical characterization of semiconductor oxide-based gas sensors using impedance spectroscopy: a review. Rev Adv Sci Eng **5**, 86–105 (2016)
62. D.K. Bandgar et al., Novel route for fabrication of nanostructured α-Fe_2O_3 gas sensor. Mater. Sci. Semicond. Process **17**, 67–73 (2014)
63. V.A. Moshnikov et al., Porous silicon with embedded metal oxides for gas sensing applications. J Non Cryst Solids **358**, 590–595 (2012)
64. J.M. Rheaume, A.P. Pisano, A review of recent progress in sensing of gas concentration by impedance change. Ionics (Kiel) **17**, 99–108 (2011)
65. S. Luo, G. Fu, H. Chen, Z. Liu, Q. Hong, Gas-sensing properties and complex impedance analysis of Ce-added WO_3 nanoparticles to VOC gases. Sol. State Electron **51**, 913–919 (2007)
66. M. Miyayama, K. Hikita, G. Uozumi, H. Yanagida, A.c. impedance analysis of gas-sensing property in CuO/ZnO heterocontacts. Sens. Actuators B Chem. **25**, 383–387 (1995)
67. N. Al-Hardan, M.J. Abdullah, A.A. Aziz, Impedance spectroscopy of undoped and Cr-doped ZnO gas sensors under different oxygen concentrations. Appl. Surf. Sci. **257**, 8993–8997 (2011)
68. V. Balasubramani et al., Highly sensitive and selective H_2S gas sensor fabricated with β-Ga_2O_3 /rGO. ECS J. Sol. State Sci. Technol. **9**, 055009 (2020)
69. S. Cui et al., Indium-doped SnO_2 nanoparticle–graphene nanohybrids: simple one-pot synthesis and their selective detection of NO_2. J. Mater. Chem. A **1**, 4462–4467 (2013)
70. D. Zhang, Z. Wu, X. Zong, Flexible and highly sensitive H2S gas sensor based on in-situ polymerized SnO_2/rGO/PANI ternary nanocomposite with application in halitosis diagnosis. Sens. Actuators B Chem. **289**, 32–41 (2019)
71. J. Chu et al., Highly selective detection of sulfur hexafluoride decomposition components H_2S and SOF_2 employing sensors based on tin oxide modified reduced graphene oxide. Carbon N Y **135**, 95–103 (2018)
72. Z. Song et al., Enhanced H_2S gas sensing properties based on SnO_2 quantum wire/reduced graphene oxide nanocomposites: equilibrium and kinetics modeling. Sens. Actuators B Chem **249**, 632–638 (2017)
73. N.S. Ramgir, Y.K. Hwang, S.H. Jhung, I.S. Mulla, J.-S. Chang, Effect of Pt concentration on the physicochemical properties and CO sensing activity of mesostructured SnO_2. Sens. Actuators B Chem. **114**, 275–282 (2006)
74. N.S.A. Eom et al., Ultrasensitive detection of low-ppm H_2S gases based on palladium-doped porous silicon sensors. RSC Adv **8**, 29995–30001 (2018)
75. B. Bhangare et al., Role of sensitizers in imparting the selective response of SnO_2/RGO based nanohybrids towards H_2S, NO_2 and H_2. Mater. Sci. Semicond. Process **105**, 104726 (2020)
76. J. Shi et al., WO_3 nanocrystals: synthesis and application in highly sensitive detection of acetone. Sens Actuators B Chem **156**, 820–824 (2011)
77. L.F. Reyes et al., Gas sensor response of pure and activated WO_3 nanoparticle films made by advanced reactive gas deposition. Sens. Actuators B Chem. **117**, 128–134 (2006)
78. Y.-S. Shim et al., Highly sensitive and selective H_2 and NO_2 gas sensors based on surface-decorated WO_3 nanoigloos. Sens. Actuators B Chem. **198**, 294–301 (2014)
79. W. Yan, M. Hu, P. Zeng, S. Ma, M. Li, Room temperature NO_2-sensing properties of WO_3 nanoparticles/porous silicon. Appl. Surf. Sci. **292**, 551–555 (2014)
80. Z. Hua, M. Yuasa, T. Kida, N. Yamazoe, K. Shimanoe, H_2 sensing mechanism of Pd-loaded WO_3 nanoparticle gas sensors. Chem. Lett. **43**, 1435–1437 (2014)
81. H. Zhou, D.-Y. Xu, H.-Q. Zuo, W. Liu, S. Lin, Preparation of flower-like Cu-WO_3 nanostructures and their acetone gas sensing performance. J. Chem. **2015**, 382087 (2015)
82. M. He et al., Highly sensitive and selective H_2S gas sensors based on flower-like WO_3/CuO composites operating at low/room temperature. J. Alloys Compd. **788**, 36–43 (2019)
83. M. Punginsang et al., Selective H_2S gas sensors based on ohmic hetero-interface of Au-functionalized WO_3 nanowires. Appl. Surf. Sci. **571**, 151262 (2022)
84. D. Feng et al., Highly sensitive and selective NiO/WO_3 composite nanoparticles in detecting H_2S biomarker of halitosis. ACS Sens. **6**, 733–741 (2021)
85. T.T.N. Hoa et al., Highly selective H_2S gas sensor based on WO_3-coated SnO_2 nanowires. Mater. Today Commun. **26**, 102094 (2021)
86. J. Shi et al., Facile synthesis of reduced graphene oxide/hexagonal WO_3 nanosheets composites with enhanced H_2S sensing properties. Sens. Actuators B Chem. **230**, 736–745 (2016)
87. M. Shahrousvand et al., Flexible magnetic polyurethane/Fe_2O_3 nanoparticles as organic-inorganic nanocomposites for biomedical applications: properties and cell behavior. Mater. Sci. Eng., C **74**, 556–567 (2017)
88. B. Shentu, T. Gan, Z. Weng, Modification of Fe_2O_3 and its effect on the heat-resistance of silicone rubber. J Appl Polym Sci **113**(5), 3202–3206 (2009)

89. E. Gerasimova, The effect of Fe_2O_3 on the mechanical properties of the polymer modified cement containing fly ash. Procedia. Eng. **150**, 1553–1557 (2016)
90. M.B. Hegde, K.N. Shetty Mohana, S.R. Nayak, A.M. Madhusudhana, Solution combustion synthesis of rGO-Fe_2O_3 hybrid nanofiller for linseed oil based eco-friendly anticorrosion coating. Colloids. Surf. A Physicochem. Eng. Asp **633**, 127863 (2022)
91. Z. Jiang et al., A high efficiency H_2S gas sensor material: paper like Fe_2O_3/graphene nanosheets and structural alignment dependency of device efficiency. J. Mater. Chem. A Mater. **2**, 6714–6717 (2014)
92. N. van Hoang et al., Excellent detection of H_2S gas at ppb concentrations using $ZnFe_2O_4$ nanofibers loaded with reduced graphene oxide. Sens. Actuators B Chem. **282**, 876–884 (2019)
93. S.-W. Choi, J.Y. Park, S.S. Kim, Growth behavior and sensing properties of nanograins in CuO nanofibers. Chem. Eng. J. **172**, 550–556 (2011)
94. A. Katoch, G.-J. Sun, S.-W. Choi, J.-H. Byun, S.S. Kim, Competitive influence of grain size and crystallinity on gas sensing performances of ZnO nanofibers. Sens Actuators B Chem **185**, 411–416 (2013)
95. T. Tao, Q. Chen, H. Hu, Y. Chen, MoO_3 nanoparticles distributed uniformly in carbon matrix for supercapacitor applications. Mater. Lett. **66**, 102–105 (2012)
96. A. Manivel et al., Synthesis of MoO_3 nanoparticles for azo dye degradation by catalytic ozonation. Mater Res Bull **62**, 184–191 (2015)
97. A. Ganguly, R. George, Synthesis, characterization and gas sensitivity of MoO_3 nanoparticles. Bull. Mater. Sci. **30**, 183–185 (2007)
98. S.-K. Shen et al., Sensing mechanism of Ag/α-MoO_3 nanobelts for H_2S gas sensor. Rare Met. **40**, 1545–1553 (2021)
99. J. Zhang et al., Enhanced trimethylamine sensing performance of single-crystal MoO_3 nanobelts decorated with Au nanoparticles. J. Alloys Compd. **685**, 1024–1033 (2016)
100. S. Zhang, Y. Zheng, P. Song, J. Sun, Q. Wang, Enhanced trimethylamine gas-sensing performance of CeO_2 nanoparticles-decorated MoO_3 nanorods. J. Mater. Sci.: Mater. Electron. **33**, 3453–3464 (2022)
101. S. Sau, S. Chakraborty, T. Das, M. Pal, Ethanol sensing properties of nanocrystalline α-MoO_3. Front Mater. **6**, 285 (2019)
102. Q.-Y. Ouyang et al., Facile synthesis and enhanced H2S sensing performances of Fe-doped α-MoO_3 micro-structures. Sens. Actuators B Chem. **169**, 17–25 (2012)
103. S. Bai, C. Chen, R. Luo, A. Chen, D. Li, Synthesis of MoO_3/reduced graphene oxide hybrids and mechanism of enhancing H_2S sensing performances. Sens. Actuators B Chem. **216**, 113–120 (2015)
104. M. Malekalaie, M. Jahangiri, A.M. Rashidi, A. Haghighiasl, N. Izadi, Selective hydrogen sulfide (H_2S) sensors based on molybdenum trioxide (MoO_3) nanoparticle decorated reduced graphene oxide. Mater. Sci. Semicond. Process **38**, 93–100 (2015)
105. H. Wang, Y. Luo, B. Liu, L. Gao, G. Duan, CuO nanoparticle loaded ZnO hierarchical heterostructure to boost H_2S sensing with fast recovery. Sens. Actuators B Chem. **338**, 129806 (2021)
106. L. Yin et al., Microwave-assisted preparation of hierarchical CuO@rGO nanostructures and their enhanced low-temperature H_2S-sensing performance. Appl Surf Sci **476**, 107–114 (2019)
107. H. Meng, W. Yang, K. Ding, L. Feng, Y. Guan, Cu_2O nanorods modified by reduced graphene oxide for NH 3 sensing at room temperature. J. Mater. Chem. A Mater. **3**, 1174–1181 (2015)
108. J.H. Kim et al., Enhancement of H_2S sensing performance of p-CuO nanofibers by loading p-reduced graphene oxide nanosheets. Sens. Actuators B Chem. **281**, 453–461 (2019)
109. N. van Hoang et al., Enhanced H_2S gas-sensing performance of α-Fe_2O_3 nanofibers by optimizing process conditions and loading with reduced graphene oxide. J. Alloys Compd. **826**, 154169 (2020)
110. N.S. Lawrence, R.P. Deo, J. Wang, Electrochemical determination of hydrogen sulfide at carbon nanotube modified electrodes. Anal. Chim. Acta. **517**, 131–137 (2004)
111. J. Fan et al., Carbon nanotubes-CuO/SnO_2 based gas sensor for detecting H_2S in low concentration. Nanotechnology **30**(47), 475501 (2019)
112. N. Kuganathan, A. Chroneos, Ru-doped single walled carbon nanotubes as sensors for SO_2 and H_2S detection. Chemosensors **9**, 120 (2021)
113. Y. Zhao, J. Zhang, Y. Wang, Z. Chen, A highly sensitive and room temperature CNTs/SnO_2/CuO sensor for H_2S gas sensing applications. Nanoscale Res. Lett. **15**(1), 1–8 (2020)
114. N. Parsafar, V. Ghafouri, A. Banaei, Electrochemical Sensing of H_2S Gas in Air by Carboxylated Multi-walled Carbon Nanotubes. J. Chem. Chem. Eng. Res. **38**, 53–62 (2019)
115. J.H. Bang et al., Decoration of multi-walled carbon nanotubes with CuO/Cu_2O nanoparticles for selective sensing of H_2S gas. Sens. Actuators B Chem. **344**, 130176 (2021)
116. S. Mubeen et al., Sensitive detection of H_2S using gold nanoparticle decorated single-walled carbon nanotubes. Anal. Chem. **82**, 250–257 (2010)
117. S. Moon et al., Co_3O_4-SWCNT composites for H_2S gas sensor application. Sens. Actuators B Chem. **222**, 166–172 (2016)
118. M. Asad, M.H. Sheikhi, M. Pourfath, M. Moradi, High sensitive and selective flexible H_2S gas sensors based on Cu nanoparticle decorated SWCNTs. Sens. Actuators B Chem. **210**, 1–8 (2015)
119. R. Hajihashemi, A.M. Rashidi, M. Alaie, R. Mohammadzadeh, N. Izadi, The study of structural properties of carbon nanotubes decorated with $NiFe_2O_4$ nanoparticles and application of nanocomposite thin film as H_2S gas sensor. Mater. Sci. Eng. C **44**, 417–421 (2014)
120. M. Asad, M.H. Sheikhi, Surface acoustic wave based H_2S gas sensors incorporating sensitive layers of single wall carbon nanotubes decorated with Cu nanoparticles. Sens. Actuators B Chem. **198**, 134–141 (2014)
121. M. Asad, M.H. Sheikhi, Highly sensitive wireless H_2S gas sensors at room temperature based on CuO-SWCNT hybrid nanomaterials. Sens. Actuators B Chem. **231**, 474–483 (2016)
122. H.Y. Jung et al., High-performance H_2S detection by redox reactions in semiconducting carbon nanotube-based devices. Analyst **138**, 7206–7211 (2013)